

# MULTIYEAR SEA ICE THICKNESS ESTIMATION USING WIDEBAND P/L-BAND RADIOMETRIC MEASUREMENTS

*Xavier Bosch-Lluis, Sidharth Misra, Carl Felten, Mehmet Ogut, Isaac Ramos-Perez, Barron Latham, Simon Yueh, Shannon Brown*

Jet Propulsion Laboratory, California Institute of Technology, Pasadena, CA 91109

## ABSTRACT

A new wideband radiometer covering P/L-band was developed at the Jet Propulsion Laboratory for polar ocean salinity and seasonal sea-ice thickness measurements. The instrument was deployed on the US Coast Guard Cutter Healy for an Arctic Ocean research cruise from September 13, 2018 to October 20, 2018. This work shows the first results relating sea ice thickness obtained from the measurements taken with the wideband P/L-band radiometer during the campaign. Results from the Arctic cruise campaign were also used to study wideband spectral properties of salinity. In addition to this paper, Salinity and wide-band calibration challenges are presented in two other companion papers.

**Index Terms**— Sea ice thickness, L-band, P-band, radiometry

## 1. INTRODUCTION

Sea ice plays an important role in regulating exchanges of heat, moisture, and salinity in the polar oceans and ultimately in the global climate. Monitoring the seasonal Arctic and Antarctic sea-ice thickness is key to understanding the heat flux between air and ocean surface as well as salt and fresh water fluxes between ocean and the frozen surfaces. There are many remote sensing technologies for the measurement of sea ice thickness, for instance NASA's second-generation Ice, Cloud, and Land Elevation Satellite (ICESat-2). ICESat-2 was launched in 2018, and will provide observations to quantify the changes in ice sheets and sea ice, and key insights into their behavior using Lidar measurements [1]. In addition; Lidar, Synthetic Aperture Radar (SAR) measurements have also been used for estimating ice concentration and thickness analysis in combination with models of sea ice thermodynamics and detection of ice motion estimated from SAR measurements [2][3].

The relationship between microwave radiometric signatures and the thickness of ice has been demonstrated in several studies using different strategies such as polarization ratios and models at different frequencies [4][5].

This work shows the preliminary and qualitative results for the Arctic sea ice thickness measurements obtained using a P-/L-band radiometer during a field campaign on board the US Coast Guard Cutter Healy (Figure 1) for an Arctic Ocean research cruise from September 13, 2018 to October 20, 18. Section 2 describes the field campaign, section 3 provides an overview of the instrument, and section 4 shows preliminary and qualitative results. We will present extended analysis at the conference. Section 5 summarizes the conclusions. Results from the Arctic cruise campaign were also used to study wideband spectral properties of salinity. In addition to this paper, Salinity and wide-band calibration challenges are presented in two companion papers.

## 2. FIELD EXPERIMENT SET-UP

The wideband P/L-band radiometer on board the US Coast Guard Cutter Healy, fig.1, was installed on September 12, 2018. The primary objective of the field campaign was to assess empirical dependence of cold-water sea surface salinity from P/L-band measurements. The expedition took 37 days to go from Dutch Harbor, Unalaska Island, AK, to the Bearing Sea, crossing the Chukchi Sea through the Bering Strait and up to the Beaufort Sea to a maximum latitude of 82° N and returning back. Figure 1, shows the pictures of the radiometer installed on the ship. The wideband radiometer was installed on the back of the cruise ship, on the left side attached to the railing and pointing to the sea surface at 45° incidence angle.

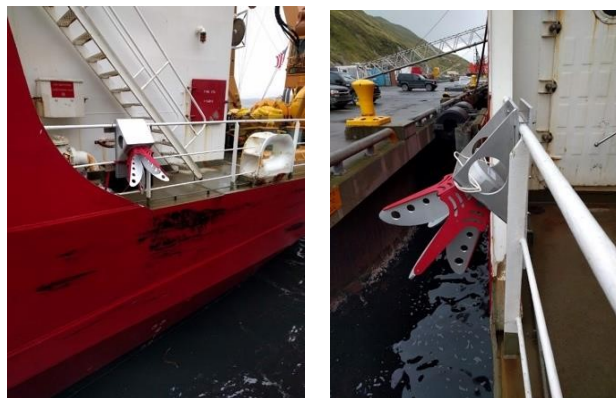


Figure 1. P/L-band antenna radiometer secured to the external railing of the U.S.C.G. Cutter Healy.

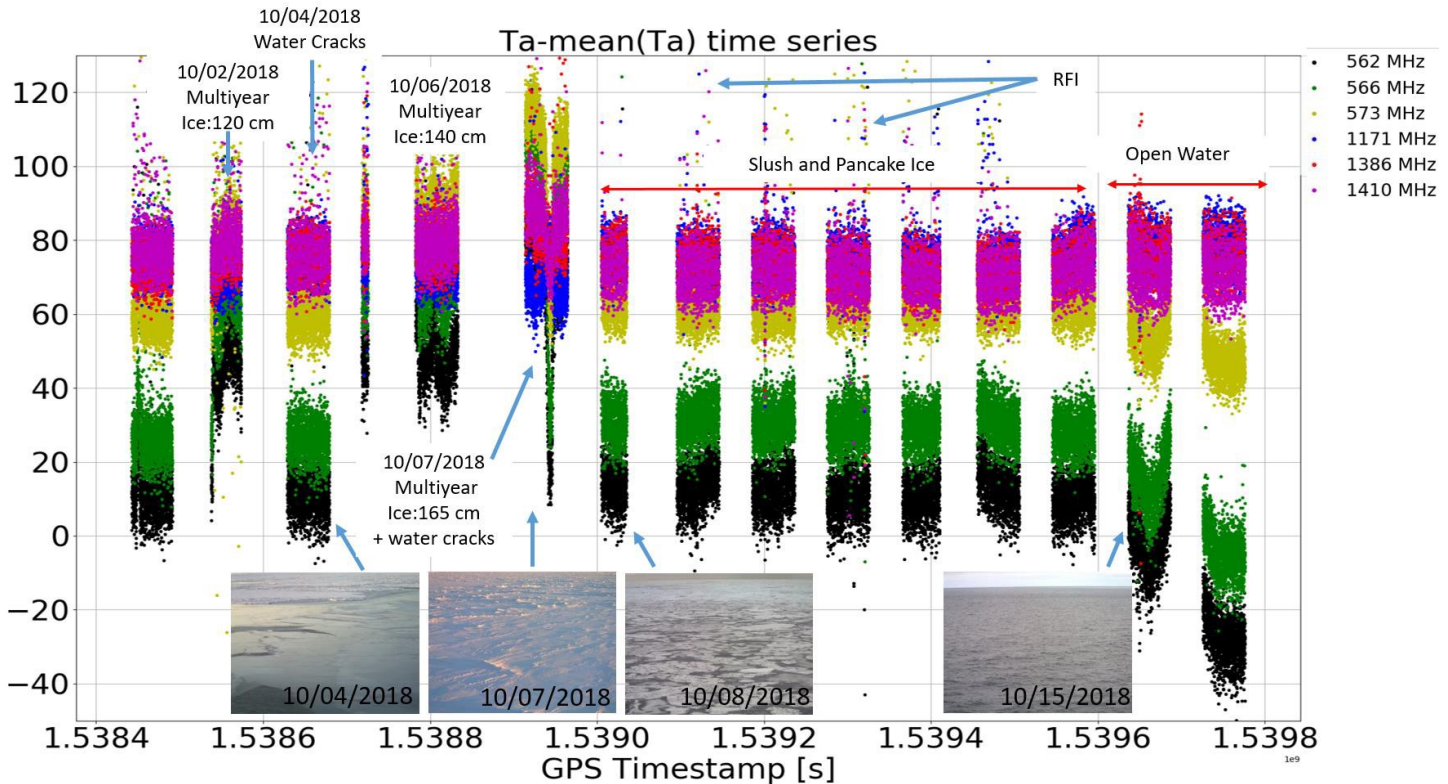


Figure 2. Time series of raw data acquired from Oct. 01 to Oct. 16 normalized to the first day for the P-/L-band radiometer on board the USCG Healy. Pictures of the measured scenes are shown, type of sea ice and mean values for the multiyear sea ice thickness are also shown.

The instrument was set to record measurements during 14 hours per day. On board of the USCG Healy there are 2 thermosalinographs recording Sea Surface Temperature (SST) and Sea Surface Salinity (SSS) every 14 seconds. In addition, ice type and thickness information were recorded in a digital log. A picture of the scene was taken every minute.

The radiometer was connected to the digital backend through a 40 feet cable. The digital backend, and data handling and control computer were inside the laboratory at room temperature.

### 3. INSTRUMENT DESCRIPTION

Technology development in the analog to digital converters (ADC) combined with current Field Programmable Gate Arrays (FPGA) allowed sampling of signals with several Gigahertz (GHz) of bandwidth. The wideband radiometer used in this work used an 8-bit ADC with a first Nyquist image at 3.2 GHz sampling rate allowing a total sampling bandwidth of 1.6 GHz. The system consists of a wideband quad-ridged antenna followed by a coupler for a noise diode input and a Dicke switch. The signal is amplified by a low

noise amplifier (LNA) and a filter bank is applied to prevent receiver saturation by Radio Frequency Interference (RFI). The filter bank can be adjusted to limit the RFI. For this experiment the filter bank was set up to allow P/L-band measurements creating two windows, one at 475-625 MHz (P-band, total 384 channels) and the other at 1050-1500 MHz (L-band, total 1154 channels). The amplified signal is sent to the digitizer for 8-bit sampling and the digitized samples are acquired by the FPGA. The FPGA calculates a 4096-channel spectrogram of the input signals using a polyphase filter and a Fast Fourier Transform (FFT) algorithm. The system temperature is around 500 Kelvin for the whole bandwidth and each channel has an individual bandwidth of 390 kHz and an integration time of 1 ms. After discarding channels with excessive RFI presence, channels are grouped and combined to reduce noise and finally antenna temperature is calculated for science applications.

### 4. DATA QUALITATIVE ANALYSIS

The time series for the radiometer measurements from Oct. 1 to Oct. 16, 2018 is presented in Figure 2. Five channels out

of the available channels have been selected, 3 P-band 542, 566, and 573 MHz, and 2 L-band, 1366 and 1410 MHz. Each channel has 3.9 MHz bandwidth (10 FFT channels averaged). The time series starts on Oct. 1 with open water measurements and all the channels have been normalized to the first day value to eliminate any offset. On Oct. 2 sea ice sheet of up to 120 cm starts showing up in the measurements. In addition, there is quite a noticeable difference between P- and L-band channels. While P-band channels are responsive to ice sheet thickness, L-band channels remain almost unchanged. On Oct. 4, the radiometer performed measurements over sea water from cracks in the ice. From Oct. 5 to Oct. 7, ice thickness has steadily increased from 120 to 165 cm, with a maximum that reached ~350 cm. From Oct. 8 to Oct. 14, the type of ice changes to slush and pancake ice with the measurement being different from multiyear ice measurements but also different from open water. Finally, on Oct. 15 and Oct. 16, the vessel was in open water, which generated a clear change on the spectral signature.

Despite the fact that the data calibration has to be refined to account for galactic noise, foam, sea roughness, time series shown in Figure 3 show dependence between multi-year sea ice thicknesses and P-band and L-band radiometric measurements. Furthermore, this dependence is higher for the P-band than for the L-band.

## 5. CONCLUSIONS

A wideband P/L-band radiometer was deployed on board the US Coast Guard Cutter Healy while cruising from the Bearing Sea to the Beaufort Sea and back with the main purpose to assess empirical dependence of cold-water sea surface salinity from P/L-band measurements. During this campaign, the vessel encountered several types of ice with multi-year ice thickness going from 120 to 350 cm. A clear relationship between multi-year ice thickness and P-band and L-band measurements was observed with the caveat that a precise calibration that accounts for galactic noise, foam, sea roughness needs to be processed to show clear results. Refined results will be presented in the conference.

## 6. ACKNOWLEDGEMENT

This research was carried out at the Jet Propulsion Laboratory, California Institute of Technology, under a contract with the National Aeronautics and Space Administration. Authors would like to thank Dr. Craig Lee from the University of Washington and the SODA (Stratified Ocean Dynamics of the Arctic) team for allowing us to install our instrument with their field campaign. We would also like to thank the crew of the U.S. Coast Guard Ship Healy for helping us install our instrument in a very short time. ©2018. California Institute of Technology. Government sponsorship acknowledged.

## REFERENCES

- [1] W. Abdalati *et al.*, "The ICESat-2 Laser Altimetry Mission," in *Proceedings of the IEEE*, vol. 98, no. 5, pp. 735-751, May 2010. doi: 10.1109/JPROC.2009.2034765
- [2] J. Karvonen *et al.*, "Bohai Sea Ice Parameter Estimation Based on Thermodynamic Ice Model and Earth Observation Data". *Remote Sensing*. 9. 234. 2017. doi: 10.3390/rs9030234.
- [3] A. Johansson *et al.*, "X-, C-, and L-band SAR signatures of newly formed sea ice in Arctic leads during winter and spring," *Remote Sensing of Environment*, Vol.204, pp. 162-180, 2018. <https://doi.org/10.1016/j.rse.2017.10.032>.
- [4] S. Martin, Drucker, R., Kwok, R., and Holt, B. "Estimation of the thin ice thickness and heat flux for the Chukchi Sea Alaskan coast polynya from Special Sensor Microwave Imager data, 1990-2001". *Journal of Geophysical Research*, 109. 2004. doi: 10.1029/2004JC002428.
- [5] S. Martin, Drucker, R., Kwok, R., and Holt, B. "Improvements in the estimates of ice thickness and production in the Chukchi Sea polynyas derived from AMSR-E". *Geophysical Research Letters*, 2005. doi: 10.1029/2004GL022013.